Applied Thermal Engineering 111 (2017) 271–279

Contents lists available at ScienceDirect

Applied Thermal Engineering

journal homepage: www.elsevier.com/locate/apthermeng

Research Paper

# Experimental investigation of the effects of using nano/phase change materials (NPCM) as coolant of electronic chipsets, under free and forced convection

Mahdieh Alimohammadi [1], Yasaman Aghli [1], Elaheh Sadat Alavi [1], Mohammad Sardarabadi *, Mohammad Passandideh-Fard

*Department of Mechanical Engineering, Ferdowsi University of Mashhad, Mashhad, Iran*

## HIGHLIGHTS

- An experimental study is performed on PCM and NEPCM as coolants of the electronic.
- Systems are compared in both free and forced convection.
- $Mn(No_3)_2$ is chosen as PCM and $Fe_3O_4$ as nanoparticle (1 wt.% of total weight).
- Steady temperature of the electronic can be decreased up to 14 °C by (NE)PCM.
- NPCM shows shorter of steady time in lower heat flux.

## ARTICLE INFO

*Article history:*
Received 1 July 2016
Revised 1 September 2016
Accepted 7 September 2016
Available online 8 September 2016

*Keywords:*
Electronic chipset cooling
Phase change materials
Nanoparticles
Temperature analysis

## ABSTRACT

In this paper, an experimental investigation is performed to study the effects of using nano/phase-change-materials (NPCM) as coolant for an electronic chipset in various scenarios that include both free and forced convection. Development of efficient cooling methods in electronic technology is significant mainly for enhancement of functionality and lifetime of electronic devices. Six different scenarios of cooling systems are conducted for an electronic chipset under various values of heat flux. The cooling scenarios include simple heat-sink (referred to HS in this paper), heat-sink that contains a phase change material (HS/PCM), and heat-sink that contains NPCM (HS/NPCM) in both free and forced convection. The PCM used in this study, $Mn(NO_3)_2$, is an inorganic salt-hydrate type; and the selected nanoparticles are $Fe_3O_4$ dispersed in the PCM by an ultrasound mechanism by a weight fraction of 1%. The steady and transient thermal behavior of the electronic chipset are investigated under different operating conditions by applying various heat fluxes from 1000 to 4000 $W/m^2$. Results show that presence of the PCM and NPCM can decrease the steady temperature of the chipset up to 14 °C and 10.5 °C compared to that of the HS for both free and forced convection, respectively. Furthermore, it is observed that the HS/PCM has better cooling and time efficiency for longer period usage whereas the HS/NPCM is preferable in temporary and intermittent use.



## 1. Introduction

By advancement in electronic technology, the size and weight of these devices have decreased while their performance significantly has been increased. The more sophisticated electronic components are applied; the more extra heat will be generated. Therefore, without an efficient thermal controlling, the heat generation and temperature fluctuations may affect the functionality and lifetime of the electronic devices.

One of the most common procedures for electronic cooling is using heat sinks linked with fans, which can increase cooling considerably by forced air circulation. In today's portable electronics, the thermal management system must be optimized to attain the highest performance in the given space and constraints. More number of fins result in more thermal exchange surface area and a better cooling. However, by increasing the number of fins in the same available space, the performance of the fans or blowers will be degraded due to less air circulation. Lohet al. [1] carried

* Corresponding author.
*E-mail address:* m.sardarabadi@yahoo.com (M. Sardarabadi).
[1] These authors have equal contribution in the paper.

http://dx.doi.org/10.1016/j.applthermaleng.2016.09.028
1359-4311/

**Nomenclature**

| | |
|---|---|
| $u$ | velocity in the x direction |
| $v$ | velocity in the y direction |
| $\rho$ | density (kg/m$^3$) |
| $\mu$ | viscosity(Pa s) |
| $\rho C_p$ | the specific heat (J/kg K) |
| $g$ | gravitational acceleration (m/s$^2$) |
| PCM | phase change material |
| HS | heat sink |
| T1 | chipset temperature |
| $\Delta T$ | temperature difference between the tip and base of the fin |
| $\beta$ | volumetric thermal expansion coefficient of the PCM 1/K |
| $P$ | pressure (Pa) |
| $T$ | temperature (K) |
| $K$ | thermal conductivity (W/m K) |
| $\varphi$ | mass fraction |
| $\rho L$ | latent heat of fusion (J/kg) |
| NPCM | nano/phase-change-material |
| NP | nanoparticle |
| T2 | heat-sink temperature |

out experimental and numerical studies to determine the optimized number of fins for a certain axial fan power.

Fan cooling is widely used for the CPU in desktop computers. Saini and Webb [2] studied and optimized fan speed and heat sink base size using two forced convection heat transfer models by an air duct and an impinging flow. Lin and Chou [3] investigated the blockage effect of axial-flow fans applied on heat sink assembly, experimentally. They put a plate at a certain distance from the top of the fan and investigated its effect on the system noise, fan performance and heat resistance. Their experimental results indicated that decreasing the flow-rate was negligible while the static-pressure loss was dramatic. Furthermore, several numerical studies were conducted for investigation of the natural and forced convection [4–7].

Phase change materials (PCM) are latent-heat storage materials that can absorb and release thermal energy in a constant temperature during the melting or freezing process. This is because of high latent heat of fusion of PCMs which provide the required temperature stability [8]. A large number of phase change materials, classified in three extended groups of organic, inorganic and eutectic, are available for various temperature range. The classification of the PCMs is shown in Fig. 1 [9].

Kandasamy et al. [10,11] investigated numerically and experimentally the use of the PCM based heat sink with various configurations contained in portable electronic packaging. The effect of heat dissipation rate, power input, thermal resistance and orientation of the packaging was studied. It was concluded that, the inclusion of the PCM in the heat sinks will increase the cooling performance during intermittent use and when the input power level is relatively high. Fok et al. [8] investigated the transient thermal performance of the heat sinks using the PCM with and without internal fins for the cooling of portable hand-held electronic devices with input power ranging from 3 to 5 W. Their experimental findings showed that the use of the PCM in the aluminum heat sink results in a better stabilized temperature and a more extended usage of the system. In addition, experimental tests were conducted by Weng et al. [12], to obtain temperature distributions of a heat pipe with the PCM for an electronic cooling system. They studied different parameters including: PCM type, PCM volume, fan speed, and input heating power. According to their study, a cooling module with the PCM can reduce power consumption of the fan and the average temperature of the heat source up to 46% and 12.3 °C, respectively. Pakrouh et al. [13] presented a numerical investigation on geometric optimization of a PCM-based pin-fin heat sinks. Number, height and thickness of the fins and the thickness of the heat sink base and different critical temperatures are studied for optimization. Baby and Balaji [14,15] carried out experimental studies to quantify the effect of heat transfer performance of a PCM based heat sinks. In their study, the effects of different types of fins are investigated for different power level ranging from 2 to 10 W. Similar studies can be seen in the works of Jaworski [16] and Mahmoud et al. [17].

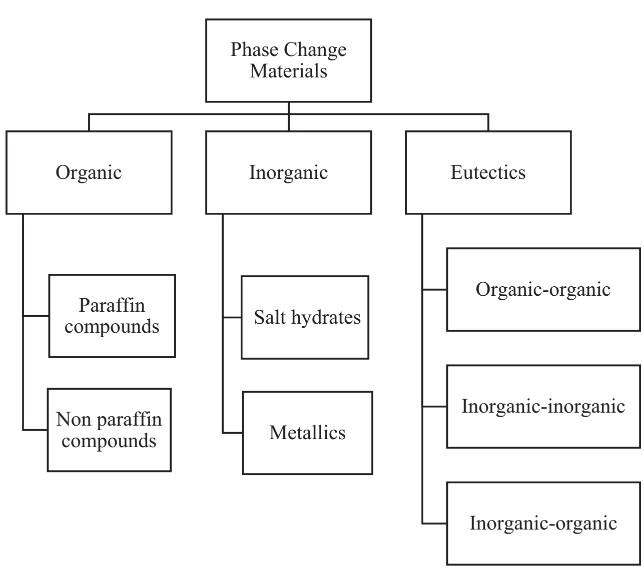


**Fig. 1.** PCMs classification.

Although the PCMs can reduce the power consumption of the system, their inherent low thermal conductivity may decrease the heat transfer rate of the system [18]. Several attempts have been made to enhance the thermal conductivity of the PCMs. Highly-conductive nano-structures may be dispersed into the PCMs to improve their effective thermal conductivity [19]. Some studies focused on identifying the thermo-physical properties of nano/phase-change-materials (NPCM) such as density, dynamic viscosity, and thermal conductivity in comparison with the pure PCMs. Ho and Gao [20], experimentally investigated the thermo-physical properties of the NPCM for use in a low temperature cool storage system. They concluded that dispersing nanoparticles in the base paraffin do not change the melting behavior of the PCM, considerably. Also, they mentioned that the nanoparticle-in-paraffin emulsion has a higher thermal conductivity (based on the nanoparticle mass fraction) in comparison with that of the pure paraffin. They found more than 2% and 6% enhancements in the thermal conductivity for the paraffin, containing 5 wt.% and 10 wt.% of nanoparticles at the temperature of 30 °C, respectively. Khodadadi et al. [21], studied numerically the natural convection solidification process of water-based nanofluid with 10% and 20%

volume fraction of copper nanoparticles in a vertical square cavity. They reported that the NPCM exhibits a higher heat release rate in comparison with the base material due to two effects: (i) increase in the thermal conductivity and (ii) reduction of the latent heat. A comprehensive 2D numerical study was conducted by Sebti et al. [22], to investigate the modification of heat transfer during the melting process of the NPCM which was paraffin-based nanofluid containing 2.5% and 5% by volume of copper nanoparticles. They concluded that the incorporation of nanoparticles leads to a decrease in the melting time. Weinstein et al. [23] experimentally studied the effect of nanoparticle weight fraction, types of graphite nanofibers (GNF), and input power level. They employed three styles of the GNF namely platelet, herringbone and ribbon style under different power levels ranged from 3 to 7 W. It is concluded that the enhancement of the thermal conductivity of the NPCM depends on the type and the mass/volume fraction of the nanoparticle, directly. For instance, the thermal conductivity of the PCM with 0.25 wt.% and 0.5 wt.% herringbone nanoparticle is 14 times and 70 times greater than pure PCM, respectively. Their study also shows that the GNFs were able to delay the steady state condition. Gharbi et al. [24] studied four configurations including pure PCM, PCM in a silicone matrix, PCM in a graphite matrix and pure PCM in a system of fins. Their results indicated that the inclusion of PCM can decrease the rising temperature of the component. Similarly, Chintakrinda et al. [25,26] conducted experimental studies to compare the transient thermal response of pure PCM, and the PCM with several thermal conductivity enhancers such as the GNF, carbon and aluminum foam and graphite nanofibers. Fan et al. [27] investigated the effects of using composite PCMs filled with high aspect-ratio carbon nano-fillers on the transient performance of a heat sink, under the various power. It is shown that the presence of the carbon nano-fillers is in general undesirable for the heating periods. However, CNT and GNP-based composite PCMs performed much better due to their greater thermal conductivity enhancement. It is found that in the solid phase, at a constant loading of 3 wt.%, the thermal conductivity of CNT-based composite PCM was only increased by 31.1%, whereas the relative enhancement was about 170% in the case of GNPs.

From the literature, fan and PCM based heat sinks are used as common methodologies for active and passive cooling of electronic equipment, respectively. Several studies have been carried out for the effects of PCM and NPCM in the cooling performance of heat sinks. A considerable number of these studies focused on paraffin as a PCM. However, few researches have focused on the salt hydrates type of the PCM. Salt hydrates have some remarkable properties compared to the paraffin such as high latent heat of fusion per unit volume, relatively high thermal conductivity (almost double of the paraffin's) and small volume changes due to melting. Furthermore, salt hydrates PCM are less corrosive, compatible with plastics, and are relatively inexpensive [9]. Therefore, in the present study, an inorganic salt-hydrate is considered as the PCM. The major drawback associated with the fan cooling method is the chipset temperature oscillation which is considered an undesirable effect of the system. Combination of a fan and a PCM, as an active and passive cooling systems, respectively, can provide simultaneous efficient cooling and temperature stability with less power consumption. In this study, various combinations of different electronic cooling systems including simple heat-sink (referred to HS in this paper), heat-sink with PCM (HS/PCM), and heat-sink with NPCM (HS/NPCM) are investigated for both free and forced convection. The experiments are performed for all six scenarios in both steady and transient operating conditions. Different operating conditions by applying various heat fluxes of an electronic chipset is examined in the experiments. Furthermore, the efficiency enhancement of the electronic chipset of the cooling systems are quantitatively investigated.

## 2. Experimental setup

In this study, the experimental setup is based on the average dimension of a common PCB (printed circuit board) as an electronic chipset. A view of the experimental setup is shown in Fig. 2. It consists of a PCB, installed on a wooden frame, a copper plate, and an aluminum heat sink. The bottom surface of the PCB is completely insulated. Details of the electronic and cooling systems can be seen in Fig. 2. In the present study, various configurations of the cooling system are investigated under free and forced convection: heat-sink cooling (HS), heat-sink PCM based (HS/PCM), and heat-sink NPCM based (HS/NPCM). In all the cases, the steady and transient operating conditions are investigated (it should be noted that the temperature is considered to reach a steady condition when the difference between eight sequential measured temperatures is less than 0.5 °C). The forced convection condition is executed by a conventional CPU fan (PBT-GF30-FR) implemented on top of the heat-sink. The heat-sink dimension is $7.5 \times 7.5 \times 4$ cm which consists of fourteen fins of 0.5 mm thickness (see Fig. 3). In the experiments, for having the maximum heat dissipation from the heat sink, the side walls of the heat sink are not insulated. For the HS/PCM and the HS/NPCM experiments, the heat-sink blades are filled by the PCM and NPCM, respectively. The selected PCM in the study, is an inorganic salt-hydrate type, $Mn(NO_3)_2$, and the selected nanoparticles are $Fe_3O_4$ dispersed in the PCM by an ultrasound mechanism by a weight fraction of 1%. The thermophysical properties of the materials are given in Table 1. The PCB with a dimension of $7.5 \times 7.5$ cm can generate a uniform heat flux up to 5000 W/m$^2$ supplied by a DC power source (30V/5A ATTEN APS3005S). In the experiments, heat-fluxes ranged from 1000 to 4000 W/m$^2$ (5.5–22.5 W) for all cooling scenarios. The values of the electrical current and voltage of input power (corresponding to different heat fluxes) are measured and saved by a multi-meter/data logger (UT71C/D/E, China).

### 2.1. Thermocouple positions

Four K-type thermocouples are mounted in four different locations of the chipset as shown in Fig. 4(a), and the average of these temperatures is reported as the chipset temperature marked by T1. Also, the heat sink temperature is measured by a K-type thermocouple at the tip of the middle fin marked by T2 and is shown in Fig. 4b. (It should be noted that the thickness of the K-type thermocouple is 0.5 mm which is lower than thickness of the fin). The measured temperatures are stored every one minute in a data logger (testo 177-T4, UK). To ensure good contact between the thermocouple tips and the copper plate, the thermocouple tips were embedded in a high thermal conductive silicone glue. Ambient temperature is measured by an alcohol thermocouple mounted in the laboratory.

### 2.2. Nanoparticles producing process

Metal oxide nanoparticles such as $Fe_3O_4$, $\gamma$-$Fe_2O_3$ and spinel-type ferrites of $MFe_2O_4$ (M refers to Mn, Co, Zn, Ni, etc.) are mostly used in different applications due to their chemical stability. These particles are produced using various methods such as chemical co-precipitation, micro-emulsion or phase transfer technique. In this study, $Fe_3O_4$ nanoparticles are generated from the chemical precipitation method by a procedure explained as follows. First of all, and before adding any salt, 200 ml of DI-water was bubbled with nitrogen gas ($N_2$) for 15 min continuously to prevent the solution from the reactions with oxygen ($O_2$). Then 5.12-g ferric chloride hex hydrate ($FeCl_3$_$H_2O$) and 2.00-g of ferrous sulfate ($FeSO_4$) were added to the water. Subsequently, the solution was stirred (by a

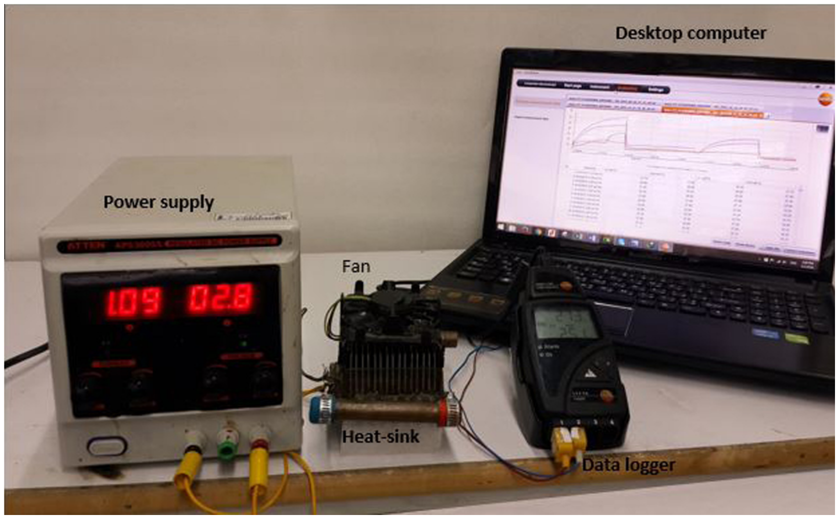


**Fig. 2.** A view of the experimental setup.

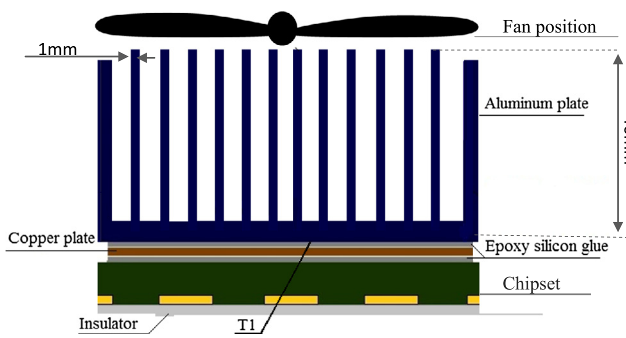


**Fig. 3.** A schematic view of the cooling system of the experimental setup.

600 rpm magnetic stirrer) and heated slowly until the solution reached to a temperature of 80 °C. Then, under nitrogen atmosphere and stirring, ammonium hydroxide ($NH_4OH$) was added drop-wise until pH exceeds 8. An acidity environment by a pH value of 5 is selected for the nanoparticle synthesis. The temperature, stirring rate, and nitrogen bubbling conditions were maintained for 2 h. Finally, the generated black $Fe_3O_4$ nanoparticles were collected by an external magnet and separated from unwanted solution of $NH_4OH$. At the end, nanoparticles were washed several times by deionized water to reach a neutral pH and dried in an oven. Furthermore, a mechanical milling process is applied for insuring that there are not any agglomerated nanoparticles (more details about the nanoparticles synthesis can be seen in [28]). Selected nanoparticles, under 40 nm in diameter (see Fig. 5), are dispersed in the PCM (Section 2.3) by 0.1 wt.%.

### 2.3. NPCM producing process

The salt hydrate is melted, after that, nanoparticles (1 wt.% by weight) are carefully mixed with the liquid salt hydrate and the mixture of NPCM is sonicated for 4 h at 60 °C by using an ultrasonic machine (Wise-Clean, WUC-D10H) to ensure proper and stable distribution of nanoparticles in the PCM. Observations show that if this mixture is stayed in the liquid phase, the nanoparticles will remain uniformly distributed within the PCM for significant durations (almost more than one week). However, after each sets of experiment the NPCM mixture is re-sonicated [16].

## 3. Thermo-physical and transport properties

The effective thermos-physical and transport properties of NPCM are directly related to properties of based PCM, nanoparticles and also volume fraction of nanoparticles. The density, specific heat, and latent of heat of fusion can be determined by the simple mixture theory. The density of an NPCM is given by:

$$\rho_C = (1-\phi)\rho_{PCM} + \phi\rho_{NP} \tag{1}$$

In this equation, the parameter of $\phi$ is the volume fraction of nanoparticle. The specific heat of the NPCM is then found:

$$(\rho C_p)_C = (1-\phi)(\rho C_p)_{PCM} + \phi(\rho C_p)_{NP} \tag{2}$$

Since the nanoparticles are assumed not to contribute to heat of fusion, the latent heat of fusion of the NPCM is evaluated as:

$$(\rho L)_C = (1-\phi)(\rho L)_{PCM} \tag{3}$$

For predicting the effective thermal conductivity of composites with spherical particles, the Maxwell's model has long been adopted [19] and verified by abundant experimental data. Therefore, the thermal conductivity of the NPCM is predicted using:

$$k_C = k_{PCM}\left[\frac{k_{NP} + 2k_{PCM} - 2\phi(k_{PCM} - k_{NP})}{k_{NP} + 2k_{PCM} + \phi(k_{PCM} - k_{NP})}\right] \tag{4}$$

And the thermal diffusivity of the NPCM is obtained via:

**Table 1**
Thermo-physical properties of the materials.

| Properties / Material | Melting Point (°C) | Heat Capacity (kJ/kg·K) | Density (kg/m$^3$) | Latent Heat kJ/kg |
|---|---|---|---|---|
| $Mn(No_3)_2$ | 37 | NA | 1540 | 115 |
| $Fe_3O_4$ | 1597 | 0.618 | 5000 | –– |

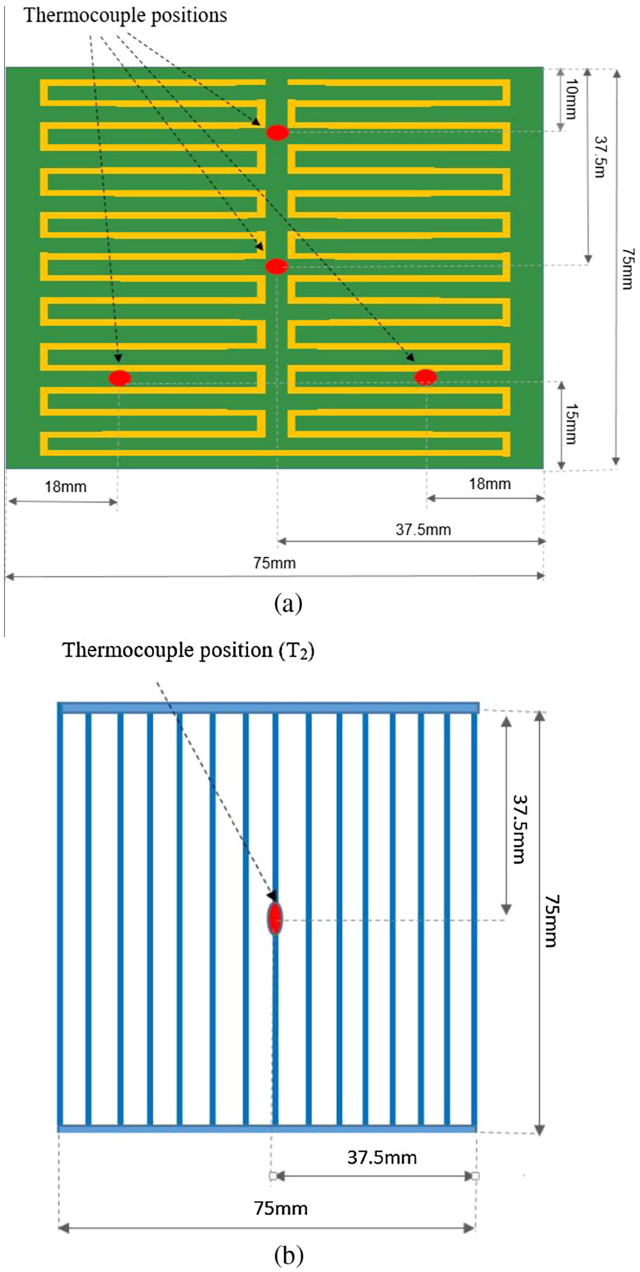


Fig. 4. Thermocouple positions of the (a) PCB and (b) the heat sink.

$$\alpha_C = \frac{k_C}{(\rho C_p)_C} \quad (5)$$

For comparison, the viscosities of the NPCM samples were also predicted using the Brinkman's correlation for concentrated suspensions, which may be given by:

$$\mu_c = \mu_{PCM}\frac{1}{(1-\phi_{Vol})^{2.5}} \quad (6)$$

It should be noted that the above equations are applied to both liquid and solid phases that have distinct properties [21].

## 4. Uncertainty analysis

Evaluation of errors in the experiments is necessary to perform a valid test. In this study, the following equation is used for this purpose:

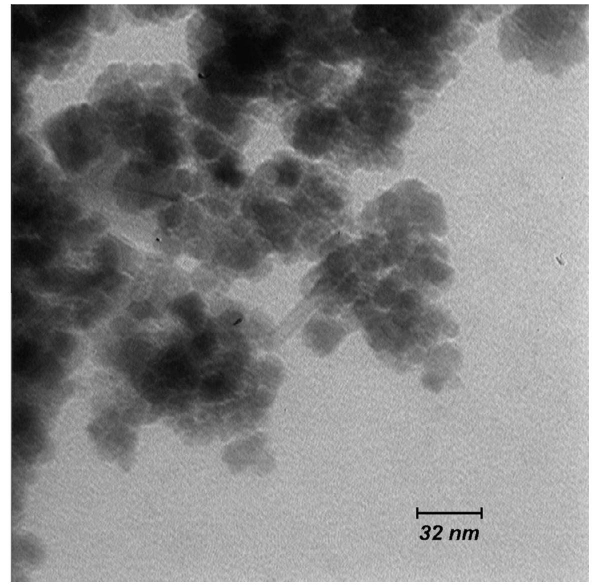


Fig. 5. Transmission electron microscopy (TEM) imaging on the dispersed nanoparticles in the PCM.

For a parameter, the total uncertainty ($\partial v$) can be related to the repetition uncertainty ($\partial v_{rep}$) and the equipment uncertainty ($\partial v_{eqp}$) as:

$$\partial v = \sqrt{(\partial v_{rep})^2 + (\partial v_{eqp})^2} \quad (7)$$

If R is a function of 'n' independent linear parameters as $R = R(v_1, v_2 \ldots v_n)$, the uncertainty of function R may be calculated as:

$$\partial R = \sqrt{\left(\frac{\partial R}{\partial v_1}\delta v_1\right)^2 + \left(\frac{\partial R}{\partial v_2}\delta v_2\right)^2 + \ldots + \left(\frac{\partial R}{\partial v_n}\delta v_n\right)^2} \quad (8)$$

The accuracy associated with the measuring instruments of the experimental setup and the maximum total uncertainty can be seen in Table 2. Thus, the maximum absolute uncertainty for all parameters was calculated to be less than 5% in the experiments which is an indication of the reliability of the measured data. Furthermore, the absolute uncertainty of the experiments in different chipset temperature is shown in Fig. 6 (HS system, 3000 W/m$^2$)

## 5. Results and discussion

In this study, experiments are carried out to investigate the effects of the PCM and NPCM as coolants for an electronic chipset with a constant heat flux. The experiments are performed in the case of free convection on three setups including heat-sink, heat-

**Table 2**
Equipment uncertainty and accuracy.

| Equipment and model | Measurement section maximum | Accuracy | Maximum uncertainty (in experiments) |
|---|---|---|---|
| Hg thermometer | Ambient temperature | ±0.5 °C | 0.288 °C |
| K-type thermocouple | Chipset temperature (T1) | ± 0.5°C | 0.306 °C |
| K-type thermocouple | Heat-sink temperature (T2) | ±0.5 °C | 0.392 °C |
| Digital multimeter (VC9805, China) | Voltage | ±0.5 V | 0.288 V |
| Digital multimeter (VC9805, China) | Ampere | ±0.8 A | 0.462 A |

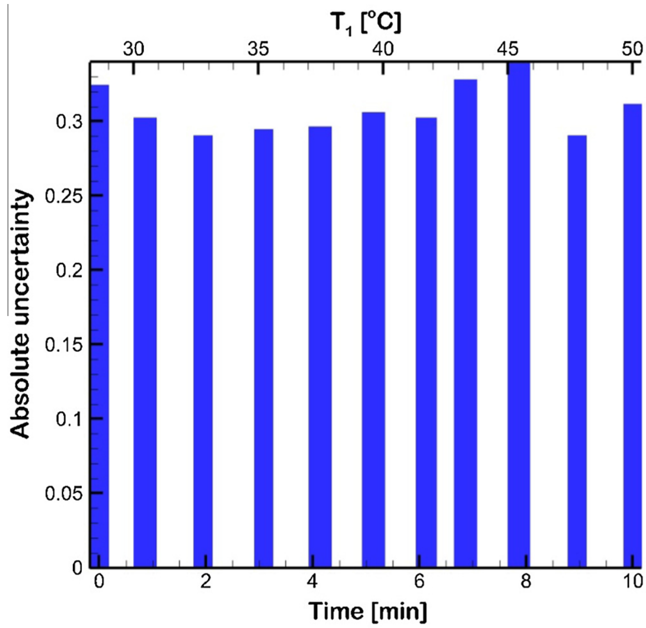


**Fig. 6.** Absolut uncertainty of the chipset transient temperature, HS system, 3000 W/m$^2$.

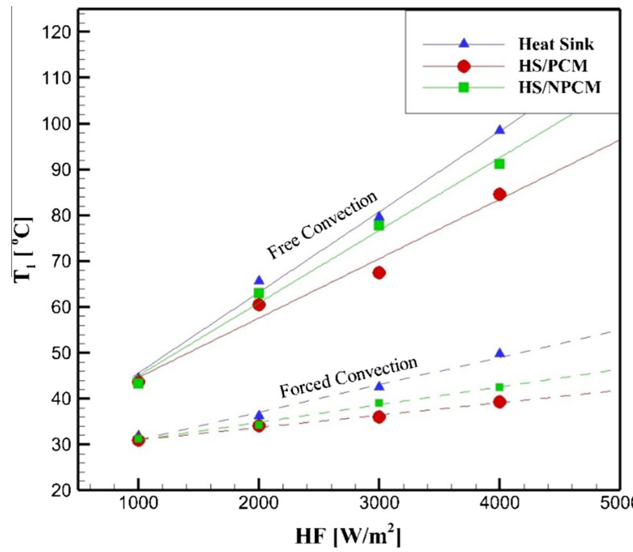


**Fig. 7.** Steady temperature of the electronic chipset for free and froced convection.

sink with PCM, and heat-sink with NPCM. Moreover, in order to investigate the effect of a complementary device on cooling enhancement, these three sets of experiments are also repeated in forced convection scenario using a fan on top of the heat sink. The selected heat-fluxes ranged from 1000 to 4000 W/m$^2$ for both free and forced convection scenarios.

### *5.1. Steady operating condition*

First set of experiments are performed to compare various cooling techniques in steady operating conditions. The chipset temperature is one of the vital parameter in the PCB operation. High temperatures and undesirable temperature changes can damage the electronic devices. Therefore, chipset temperature can be an essential criterion to examine whether a cooling system works properly. Thus, this temperature data is collected in different experiments.

The steady temperature of the PCB (T1) as a function of heat-flux for both free and force convection is shown in Fig. 7. The temperature is considered to reach a steady condition when the difference between eight sequential measured temperatures is less than 0.5 °C. As seen in Fig. 7, for heat-fluxes higher than 3000 W/m$^2$, the HS/PCM and HS/NPCM can reduce the chipset temperature considerably compared to that of the heat sink with no extra cooling medium (HS) for both free and forced convection scenarios. For a heat flux of 4000 W/m$^2$, the HS/PCM has a maximum temperature reduction of 14 °C and 10.5 °C compared to that of the HS in free and forced convection scenarios, respectively. The main reason for this temperature reduction is increasing the heat capacity of the system when a PCM is used. From Fig. 7, it can also be seen that for a heat-flux of 1000, the effect of the cooling method on the chipset temperature is negligible. This is because at small heat fluxes the temperature gradient in the system is small and in all cooling systems the steady temperature is almost equal. Moreover, it can be seen that cooling enhancement of the PCM by adding $Fe_3O_4$ nanoparticles (i.e., the HS/NPCM) is slightly lower than the pure PCM (HS/PCM). This can be explained by the fact that the heat capacity of the NPCM is lower than that of the PCM. From Fig. 7, it can be inferred that simultaneous using of fan cooling and HS/PCM shows the best cooling enhancement in comparison with other cases.

The temperature difference between the tip and base of the fin in the heat sink ($\Delta T$) can be used as an indicator for the amount of heat removed from the chipset. A smaller value of $\Delta T$ shows a better heat transfer and consequently a more efficient cooling method. The $\Delta T$ as a function of heat-flux is displayed in Fig. 8a and b for both free and forced convection, respectively. It can be seen from both Fig. 8a and b, the $\Delta T$ as a function of heat flux has nearly a linear and upward trend. The presence of PCM and NPCM through the heat sink blades results in $\Delta T$ reduction and consequently a cooler chipset temperature. The slope of $\Delta T$ vs. the heat flux is approximately 3 °C per 1000 W/m$^2$ for the HS in free convection. This slope for the HS/PCM is around 2.0 °C per 1000 W/m$^2$; i.e. a reduction of nearly 33% compared to that of the HS. A close inspection of Fig. 8 shows that the reduction for the HS/NPCM system compared to that of the HS is around 17%. Similarly, in forced convection for the HS/PCM and HS/NPCM, the reduction of the slope of $\Delta T$ vs. the heat flux compared to that of the HS is nearly 38% and 19%, respectively.

### *5.2. Temperature evolution of the electronic chipset*

For further investigation of the thermal behavior of the cooling system, the transient time evolution of the chipset temperature was also studied in this paper. Fig. 9 shows temperature-time response of the same six scenarios for experiments at a heat flux of 3000 W/m$^2$. It can be observed in the figure that the transient chipset temperature is considerably decreased in presence of the PCM and NPCM especially during the melting process. For instance, in free convection cooling (Fig. 9a), after 28 min elapsed from the heating, for both HS/PCM and HS/NPCM systems, the chipset temperature is approximately 30 °C cooler than that of the HS. Fig. 9a also indicates a significant difference in thermal behavior between the PCM and NPCM systems. In fact, up to the end of the NPCM melting phase (28 min), the HS/NPCM shows a better thermal performance because it keeps the chipset average temperature 4 °C cooler than that of the PCM. After the melting phase (28 min), however, the HS/PCM is thermally more efficient since it results in a lower operating temperature (T1). Thus, the HS/NPCM is more adequate for temporary and intermittent usage such as electronic

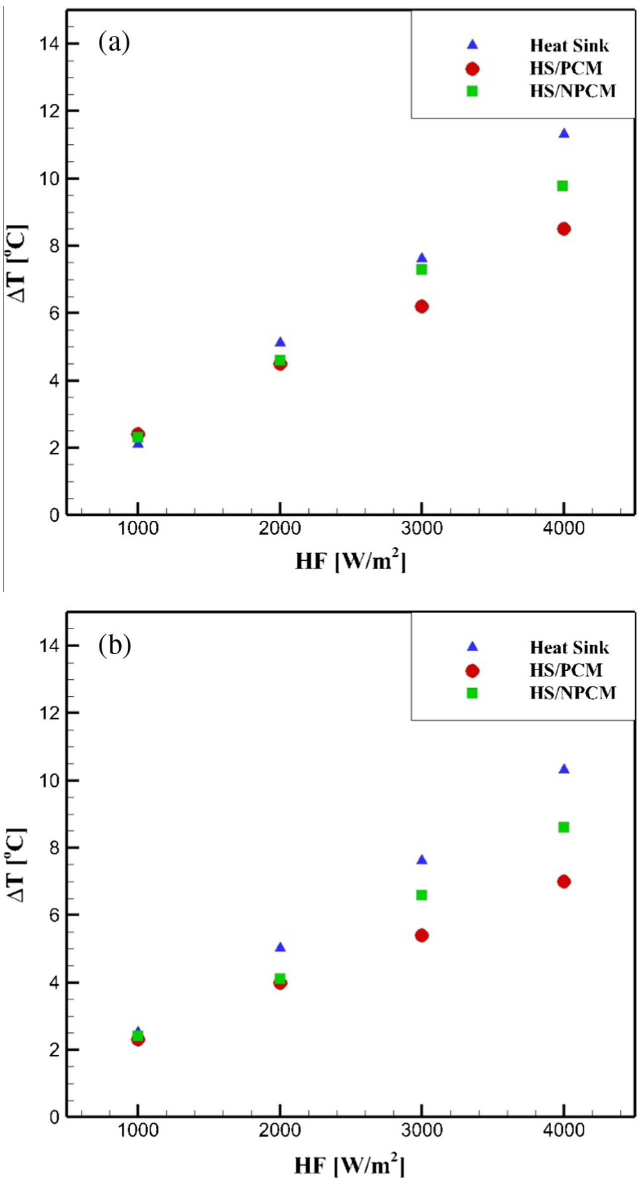


**Fig. 8.** Temperature difference between the tip and base of the fin (a) free convection, (b) forced convection.

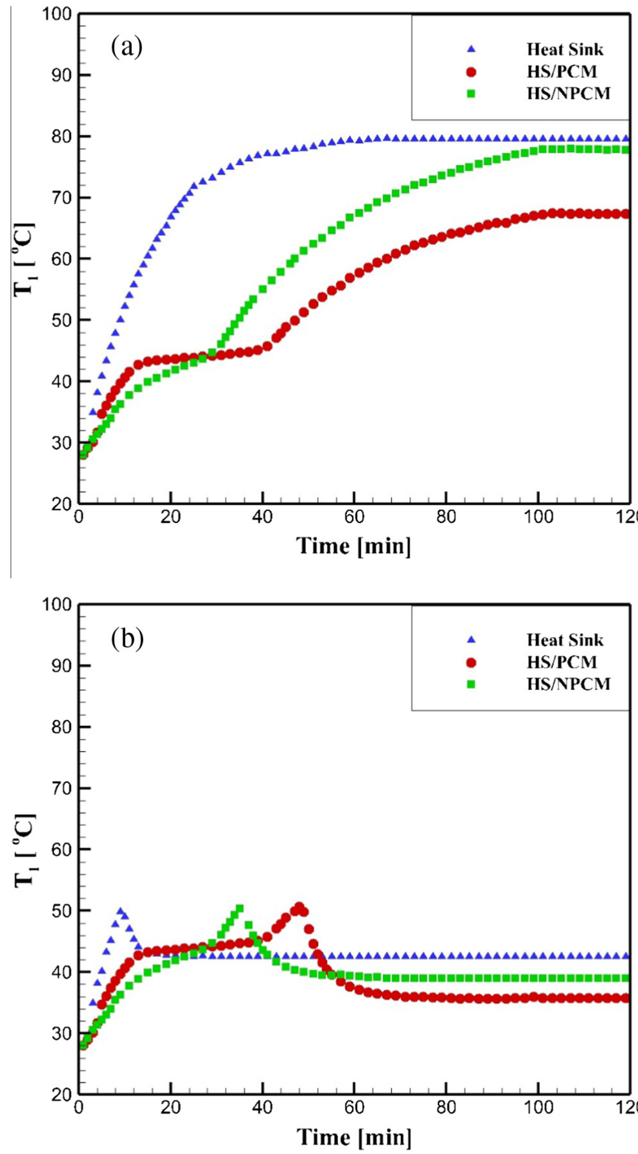


**Fig. 9.** Temperature-time response of the electronic chipset at 3000 W/m$^2$ (a) free convection, (b) forced convection.

chipsets used in household devices, whereas for applications concerning long term and continuous cooling, the HS/PCM provides a better thermal performance.

Another result of the Fig. 9a is that in the HS system without any PCM, the temperature rises to the steady condition more rapidly; i.e., T1 reaches the steady value in around 60 min. When employing the PCM along with the HS, the steady state temperature is reached after nearly 100 min for both the HS/PCM and NPCM cooling systems. Hence, using the PCM delays the steady state temperature as much as 40 min mainly due to melting process.

Fig. 9b illustrates the time evolution of temperature profiles at a heat flux of 3000 W/m$^2$ for the forced convection cases. It should be noted the critical operating temperature (a temperature where the fan is turned on) is different for electronic equipment depending on their applications. In this research, the critical chipset temperature is set at 50 °C. The figure shows the starting time of the fan cooling is delayed by around 40 min. and 26 min. for the HS/PCM and HS/NPCM compared to that of the HS, respectively. Thus, using the PCM reduces the amount of power consumption and also provides less acoustic noise and system vibration.

### 5.3. Operating time

Another significant parameter in terms of electronics thermal performance is the time it takes for the system to reach a certain temperature. A better cooling of the system will delay this time. Fig. 10a and b compares the time it takes for the PCB to reach to the set point temperature of 35 °C and 45 °C at various heat fluxes, respectively. The same results along with the time needed for the PCM to melt are also listed in Table 2. The results indicated that adding PCM or NPCM in the cooling system plays a major role in delaying the system to reach a certain temperature mainly due to the melting process at which the chipset temperature is nearly constant.

It can be seen in Table 3 that for the PCM, the melting duration is considerably higher compared to that of the NPCM at a low heat flux of 1000 W/m$^2$. However, by increasing the heat flux to 3000 W/m$^2$, the PCM and NPCM melting duration difference

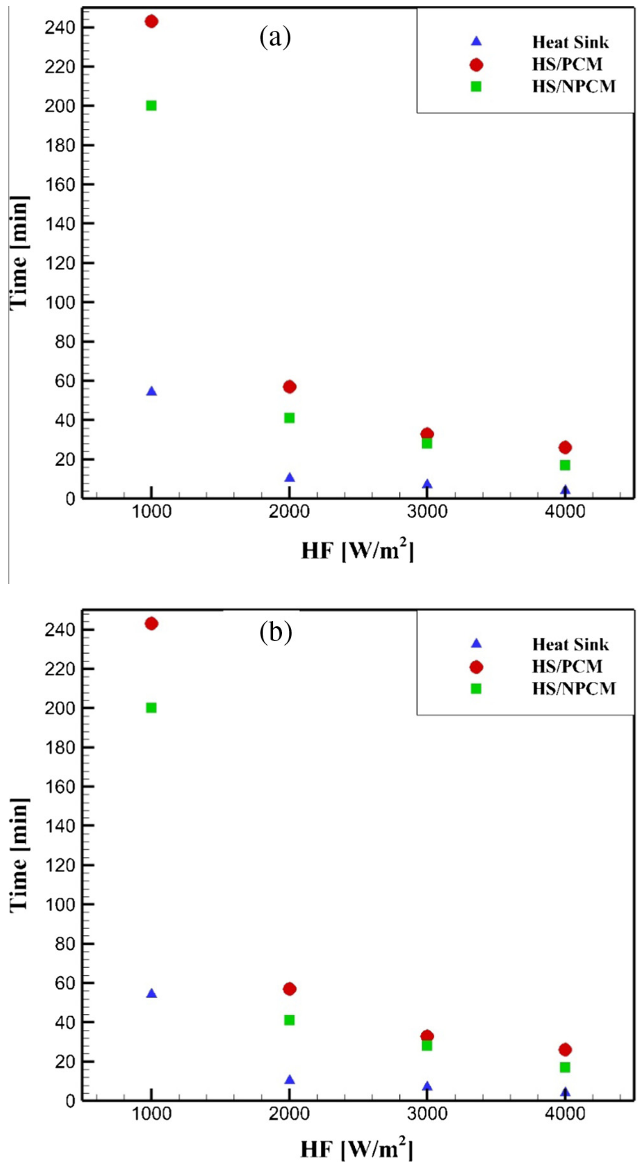


**Fig. 10.** Taken time to reach to the set point temperatures of (a)35 °C, (b)45 °C.

becomes negligible (it should be noted that melting process is considered as a time period which temperature variation of the PCM is less than 0.5 °C). Based on the experiments the required time for the electronic chipset to raise to the set point temperature of 35 °C is considerably more for the HS/PCM and HS/NPCM compared to that of the heat-sink with no extra cooling medium. For the heat flux of 1000 and 2000 W/m$^2$ the HS/NPCM has the maximum operating time as high as 40 and 11 min, respectively. Since the melting process of PCM and NPCM does not start during this period, the thermal energy is stored in the form of sensible heat. Therefore, the amount of stored heat depends on the specific heat parameter of the medium, the temperature changes and the amount of PCM material. Adding $Fe_3O_4$ nanoparticles to the PCM increased the specific heat, significantly. Therefore, as it is shown in Fig. 10a, the HS/NPCM has a better time enhancement than that of the HS/PCM for a heat flux of 1000 and 2000 W/m$^2$. However, in the heat flux of 3000 and 4000 W/m$^2$, temperature rises rapidly which results in a negligible difference in time enhancement for the PCM and NPCM. The time duration for the electronic chipset to reach 45 °C is seen in Fig. 10b; this time includes the duration for both sensible and latent heat mechanisms. Up to 35 °C, the heat storage is related to the sensible heat, whereas in following trend to reach 45 °C , the latent heat storage starts when PCM and NPCM undergoes a phase change from solid to liquid. Thus, in analyzing the chipset temperature to reach 45 °C, the amount of latent heat should be considered in order to compare the performance of PCM and NPCM with regard to time enhancement. Considering the fact that the presence of nanoparticles into the PCM reduces the latent heat [29], it can be seen in Fig. 10b that for all tested heat fluxes, less time is taken for the NPCM to reach 45 °C compared to the PCM. In heat flux of 1000 W/m$^2$, the HS/PCM experiences the longest operating time as long as 243 min which is 4.5 times longer than that of a conventional heat sink.

### 5.4. Efficiency enhancement of the chipset

A significant parameter for evaluating the electronic function of a chipset is the amount of its power consumption. Therefore, to compare different cooling methods of the chipset, the one which reduces more power consumption, can be considered to be more efficient. In other words, more reduction of the power consumption can be regarded as more heat dissipation which translates in the system to be more efficient. Consequently, to evaluate the performance of the cooling systems including HS, HS/PCM and HS/NPCM, three extra sets of experiments were carried out. The heat flux was initially set at 3000 W/m$^2$ and the transient variation of power consumption of the chipset was recorded. Fig. 11 demonstrates the evolution of the power consumption as a function of time for three mentioned cooling methods. The results from the figure indicate that the HS, HS/PCM and HS/NPCM cooling systems can reduce the power consumption of the electronic chipset in comparison with a chipset with no cooling system by 4.33%,

**Table 3**
Operating time of the study cases for different heat fluxes.

| Heat flux (W/m$^2$) | | Time that the chipset temperature reach to 35 (min) | Melting duration (min) | Time that the chipset temperature reach to 45 (min) |
|---|---|---|---|---|
| 1000 | Heat Sink | 10 | | 54 |
| | HS/PCM | 25 | 100 | 243 |
| | HS/NPCM | 40 | 70 | 200 |
| 2000 | Heat Sink | 3 | | 10 |
| | HS/PCM | 7 | 35 | 57 |
| | HS/NPCM | 11 | 30 | 41 |
| 3000 | Heat Sink | 2.5 | | 7 |
| | HS/PCM | 6 | 30 | 33 |
| | HS/NPCM | 5 | 25 | 28 |
| 4000 | Heat Sink | 1.5 | | 4 |
| | HS/PCM | 5.5 | 20 | 26 |
| | HS/NPCM | 4 | 16 | 17 |

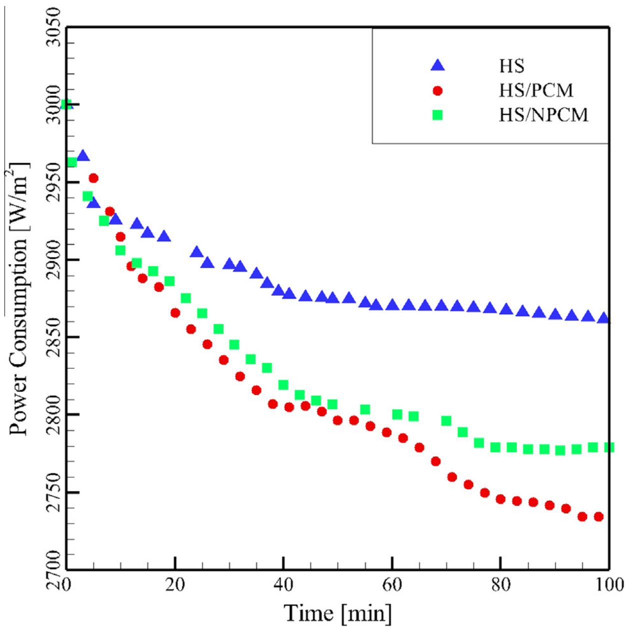


**Fig. 11.** Transient variation of the power consumption of the chipset.

8.83% and 7.33%, respectively. However, it can be observed that the transient power consumption is decreased significantly, in the HS/PCM and HS/NPCM compared to that of the HS. For example, the power consumption of the chipset is approximately 70 W/m$^2$ lower than that of the HS at 60 min from the start, for both HS/PCM and HS/NPCM.

## 6. Conclusion

In this study, three cooling systems of simple heat-sink (HS), heat-sink that contains a phase change material (HS/PCM), and heat-sink that contains NPCM (HS/NPCM) for an electronic chipset are conducted experimentally in both free and forced convection. Important operating parameters for an electronic chipset such as the steady temperature, the temperature-time response and the operating time analysis are evaluated to attain the most efficient thermal performance. The results indicate that in the cooling system with the PCM the steady temperature of the chipset has a maximum reduction of 14 °C and 10.5 °C compared to that of the HS for a heat flux of 4000 W/m$^2$ for both free and forced convection, respectively. Furthermore, the presence of PCM and NPCM delayed the steady state condition of the chipset significantly in free convection. For forced convection, the start of the fan cooling is delayed which results in less power consumption as well as noise reduction. For the electronic chipset with power inputs less than 2000 W/m$^2$ especially for the temporary and intermittent use, the HS/NPCM is preferred because of the maximum operating time compared to that of HS and HS/PCM. While, for the chipset with input power higher than 3000 W/m$^2$ and longer usage time, the HS/PCM has better cooling and time efficiency compared to the other cooling systems.

## References


[1] C.K. Loh, D. Nelson, D.J. Chou, Thermal characterization of fan-heat sink systems in miniature axial fan and micro blower airflow, in: Semiconductor Thermal Measurement and Management, 2001. Seventeenth Annual IEEE Symposium, 2001, pp. 111–116.

[2] M. Saini, R.L. Webb, Heat rejection limits of air cooled plane fin heat sinks for computer cooling, IEEE Trans. Compon. Packag. Technol. 26 (2003) 71–79.

[3] S.-C. Lin, C.-A. Chou, Blockage effect of axial-flow fans applied on heat sink assembly, Appl. Therm. Eng. 24 (11) (2004) 2375–2389.

[4] H. Shokouhmand, S.M.A. Noori Rahim Abadi, A. Jafari, The effect of the horizontal vibrations on natural heat transfer from an isothermal array of cylinders, Int. J. Mech. Mater. Des. 7 (2011) 313–326.

[5] Investigation of Mixed Convection in a Vertical Microchannel Affected by EDL, presented at the World Congress on Engineering, London, U.K., 2010.

[6] M.R.A. Jafari, A. Saeedmanesh, An unsteady mixed convection in a driven cavity filled with nanofluids using an externally oscillating, J. Electron. Cool. Therm. Control 3 (2013) 58–73.

[7] S.M.A.N.R. Abadi, A. Jafari, Investigating the natural convection heat transfer from two elliptic cylinders in a closed cavity at different cylinder spacings, Heat Transf. Res. 43 (2012).

[8] S.C. Fok, W. Shen, F.L. Tan, Cooling of portable hand-held electronic devices using phase change materials in finned heat sinks, Int. J. Therm. Sci. 49 (1) (2010) 109–117.

[9] A. Sharma, V.V. Tyagi, C.R. Chen, D. Buddhi, Review on thermal energy storage with phase change materials and applications, Renew. Sustain. Energy Rev. 13 (2) (2009) 318–345.

[10] R. Kandasamy, X.-Q. Wang, A.S. Mujumdar, Application of phase change materials in thermal management of electronics, Appl. Therm. Eng. 27 (12) (2007) 2822–2832.

[11] R. Kandasamy, X.-Q. Wang, A.S. Mujumdar, Transient cooling of electronics using phase change material (PCM)-based heat sinks, Appl. Therm. Eng. 28 (6) (2008) 1047–1057.

[12] Y.-C. Weng, H.-P. Cho, C.-C. Chang, S.-L. Chen, Heat pipe with PCM for electronic cooling, Appl. Energy 88 (5) (2011) 1825–1833.

[13] R. Pakrouh, M.J. Hosseini, A.A. Ranjbar, R. Bahrampoury, A numerical method for PCM-based pin fin heat sinks optimization, Energy Convers. Manage. 103 (10) (2015) 542–552.

[14] R. Baby, C. Balaji, Experimental investigations on phase change material based finned heat sinks for electronic equipment cooling, Int. J. Heat Mass Transf. 55 (2) (2012) 1642–1649.

[15] R. Baby, C. Balaji, Thermal performance of a PCM heat sink under different heat loads: an experimental study, Int. J. Therm. Sci. 79 (5) (2014) 240–249.

[16] M. Jaworski, Thermal performance of heat spreader for electronics cooling with incorporated phase change material, Appl. Therm. Eng. 35 (3) (2012) 212–219.

[17] S. Mahmoud, A. Tang, C. Toh, R. Al-Dadah, S.L. Soo, Experimental investigation of inserts configurations and PCM type on the thermal performance of PCM based heat sinks, Appl. Energy 112 (12) (2013) 1349–1356.

[18] W.R. Humphries, E.I. Griggs, A design handbook for phase change thermal control and energy storage devices, N-78-15434; NASA-TP-1074; M-230 United States Fri Feb 08 07:47:48 EST 2008NTIS PC A12/MF A01.ERA-04-003579; EDB-79-002261English, 1977.

[19] L. Fan, J.M. Khodadadi, A theoretical and experimental investigation of unidirectional freezing of nanoparticle-enhanced phase change materials, J. Heat Transf. 134 (2012) 092301.

[20] C.J. Ho, J.Y. Gao, Preparation and thermophysical properties of nanoparticle-in-paraffin emulsion as phase change material, Int. Commun. Heat Mass Transf. 36 (5) (2009) 467–470.

[21] J.M. Khodadadi, S.F. Hosseinizadeh, Nanoparticle-enhanced phase change materials (NEPCM) with great potential for improved thermal energy storage, Int. Commun. Heat Mass Transf. 34 (5) (2007) 534–543.

[22] S.S. Sebti, M. Mastiani, H. Mirzaei, A. Dadvand, S. Kashani, S.A. Hosseini, Numerical study of the melting of nano-enhanced phase change material in a square cavity, J. Zhejiang Univ. Sci. A 14 (2013) 307–316.

[23] R.D. Weinstein, T.C. Kopec, A.S. Fleischer, E. D'Addio, C.A. Bessel, The experimental exploration of embedding phase change materials with graphite nanofibers for the thermal management of electronics, J. Heat Transf. 130 (2008) 042405.

[24] S. Gharbi, S. Harmand, S.B. Jabrallah, Experimental comparison between different configurations of PCM based heat sinks for cooling electronic components, Appl. Therm. Eng. 87 (2015) 454–462, 8/5/ 2015.

[25] K. Chintakrinda, R.J. Warzoha, R.D. Weinstein, A.S. Fleischer, Quantification of the impact of embedded graphite nanofibers on the transient thermal response of paraffin phase change material exposed to high heat fluxes, J. Heat Transf. 134 (2012) 071901.

[26] K. Chintakrinda, R.D. Weinstein, A.S. Fleischer, A direct comparison of three different material enhancement methods on the transient thermal response of paraffin phase change material exposed to high heat fluxes, Int. J. Therm. Sci. 50 (9) (2011) 1639–1647.

[27] L.-W. Fan, Z.-Q. Zhu, Y. Zeng, Y.-Q. Xiao, X.-L. Liu, Y.-Y. Wu, et al., Transient performance of a PCM-based heat sink with high aspect-ratio carbon nanofillers, Appl. Therm. Eng. 75 (2012) 532–540, 1/22/2015.

[28] M. Ghadiri, M. Sardarabadi, M. Pasandideh-fard, A.J. Moghadam, Experimental investigation of a PVT system performance using nano ferrofluids, Energy Convers. Manage. 103 (10) (2015) 468–476.

[29] M. Li, A nano-graphite/paraffin phase change material with high thermal conductivity, Appl. Energy 106 (6) (2013) 25–30.